Analyzing the Real Advantages of Bifunctional Initiator over Monofunctional Initiator in Free Radical Polymerization

Paula F. de M. P. B. Machado, Liliane M. F. Lona

School of Chemical Engineering, University of Campinas, UNICAMP, Campinas-SP 13083-970, Brazil

Received 24 July 2008; accepted 27 December 2009
DOI 10.1002/app.32010
Published online 27 April 2010 in Wiley InterScience (www.interscience.wiley.com).

ABSTRACT: Monofunctional initiators are extensively used in free radical polymerization. To enhance productivity, a higher temperature is usually used; however, this leads to lower molecular weights. Bifunctional initiators can increase the polymerization rate without decreasing the average molecular weight and this can be desirable. A bifunctional initiator is an important issue to be investigated, and it is of great interest to industries. The objective of this work is to study polymerization reactions with mono- and bi-functional initiators through comprehensive mathematical models. Polystyrene is considered as case study. This work collects and presents some experimental data available in literature for polymerization using two different types of bifunctional initiators. Model prediction showed good agreement with experimental data. It was observed that the initial initiator concentration has a huge impact on the efficiency of initiators with functionality bigger than one and high concentrations of bifunctional initiator make the system behave as if it were a system operating with monofunctional initiator. © 2010 Wiley Periodicals, Inc. J Appl Polym Sci 117: 2803–2816, 2010

Key words: polymerization; monofunctional initiator; bifunctional initiator; styrene; reactor; simulation

INTRODUCTION

Monofunctional peroxides are extensively used in industries for the production of many kinds of polymers as can be seen in Gao and Penlidis[1] and in industrial initiators catalogues. This type of initiator produces two free radicals for each decomposed molecule of initiator. To enhance productivity, usually higher temperature or higher initiator concentration are used. However, both alternatives lead to lower molecular weights.

Research institutes and chemical industries strive to explore bifunctional initiators because they are known as substances that increase the polymerization rate without decreasing the average molecular weight. Such initiators are decomposed into three fragments: one of them, called diradical, has two free radicals (one at each end), which allows the chain to grow on both sides of the fragment, thus increasing the reaction rate with no decrease in molecular weight. Some studies with polystyrene using mono- and bi-functional initiators are found in literature,[2–13] showing important results mostly regarding conversion and molecular weights and presenting the performances of these two types of initiator with no comparisons in the same charts. Table I presents a short summary of these important works.

In this present work, styrene was chosen as study case as there are a lot of data about it in literature and because the focus of this work was the functionality of initiators and not different types of monomer, so it was logical to choose a well-known monomer.

In this work, it was, for the first time, observed that the efficiency of bifunctional initiator is not always superior when compared to the monofunctional initiator. It depends on the operating conditions used (temperature and initiator concentration). Results from a monofunctional initiator (BPO – dibenzoyl peroxide) and a bifunctional initiators (L256 – 2,5-dimethyl-2,5-bis(2-ethyl hexanoyl peroxy) hexane and D162 – 1,4-bis(t-butylperoxy carbo)cyclohexane cyclohexane) are presented together in the same chart, under different operating conditions to highlight the differences in performance between them and to verify the real advantages of each initiator in comparison to the others depending on the operating condition.

The model used in this work provides, besides molecular weights and conversion, a variety of results like profiles of initiator concentration, radical concentration, polydispersity index, radical concentration of different species of living polymer (λ_i, $\widetilde{\lambda}_i$) and dead polymer (μ_i, $\widetilde{\mu}_i$, $\widetilde{\widetilde{\mu}}_i$) promoting a better understanding of the polymerization system.

Correspondence to: L. M. F. Lona (liliane@feq.unicamp.br).

TABLE I
Published Literature About Bifunctional Initiators

Work	Approach
Choi and Lei[2]	Development of a model for styrene free radical polymerization, using a symmetrical bifunctional initiator (Diperoxyester). The paper shows results regarding conversion and molecular weights and MWD.
Choi et al.[3]	Development of a model for styrene free radical polymerization, using a symmetrical bifunctional initiator (2,5-dimethyl-2,5-bis(benzoyl peroxy) hexane). The paper shows results regarding polymerization rate and molecular weights.
Kim et al.[4]	Development of a model for styrene free radical polymerization, using a unsymmetrical bifunctional initiator (4-((tert-butylperoxy) carbonyl)-3-hexyl-6-([7-((tert-butylperoxy) carbonyl)heptyl]cyclohexene)). The paper shows results regarding polymerization rate, molecular weights and a discussion about the initiator efficiency.
Villalobos et al.[5]	Development of a model for styrene free radical polymerization, using three bifunctional initiators (D162, L33180B e L256). The paper shows results regarding conversion, molecular weights, MWD and a small discussion about the comparison with monofunctional initiator BPO.
Yoon and Choi, 1992[6]	Development of a model for styrene free radical polymerization, using a symmetrical bifunctional initiator (2,5-dimethyl-2,5-bis(2-ethyl hexanoyl peroxy)hexane). The paper shows results regarding the effects of temperature and initiator concentration on polymerization rate and molecular weights and a discussion about the initiator efficiency.
Yoon and Choi[7]	Development of a model for styrene free radical polymerization, using a binary mixture of symmetrical bifunctional initiators. The paper shows results regarding polymerization rate, molecular weights and a comparison with a monofunctional initiator model.
Gonzalez et al.[8]	Development of a model for styrene free radical polymerization, using a mixture of mono- and bi-functional initiators. The paper shows results regarding polymerization rate, molecular weights and comparisons between the behavior of the mixture and monofunctional initiators only.
Dhib et al.[9]	Development of a model for styrene free radical polymerization, using a variety of bi- and mono-functional initiators. The paper shows results regarding conversion, molecular weights and discussions about the behavior of each initiator presented.
Cavin et al.[10]	Development of a model for styrene free radical polymerization, using bifunctional initiator L256. The paper shows results regarding, polymerization rate, conversion, molecular weights, polydispersity index and a discussion about the initiator efficiency.
Benbachir and Benjelloun[11]	Development of a model for styrene free radical polymerization, using bifunctional initiators (Diperoxyesters). The paper shows results regarding the effects of temperature and initiator concentration on conversion and molecular weights, polydisperity index, MWD and a small discussion about the comparison with monofunctional initiators.
Dhib and Al-Nidawy[12]	Development of a model for ethylene free radical polymerization, using bifunctional initiators. The paper shows results regarding the effects of temperature on conversion, conversion, molecular weights, polydispersity index and a discussion about the initiator efficiency.
Asteasuain et al.[13]	Development of a model for styrene polymerization, using asymmetric bifunctional initiators. The paper shows results regarding the effects of temperature and initiator concentration on conversion, molecular weights and MWD profiles.

REACTION MECHANISM AND MATHEMATICAL MODEL

The reaction mechanisms for the free radical polymerization of styrene using mono- and bi-functional initiator are summarized below.

Monofunctional initiator

Initiation

$$I \xrightarrow{k_d} 2R^*_{\text{in}} \tag{1}$$

$$R^*_{in} + M \xrightarrow{k'_p} R^*_1 \tag{2}$$

$$3M \xrightarrow{k_{\text{ia}}} 2R^*_1 \tag{3}$$

Propagation

$$R^*_r + M \xrightarrow{k_p} R^*_{r+1} \tag{4}$$

Termination
Combination

$$R^*_r + R^*_s \xrightarrow{k_{tc}} P_{r+s} \tag{5}$$

Chain Transfer to Small Molecules

$$R^*_n + T \xrightarrow{k_{fT}} P_r + T^* \tag{6}$$

T = initiator, solvent, CTA, inhibitor or impurity

Bifunctional initiator

Initiation

$$I \xrightarrow{2k_{d1}} R^*_{\text{in}} + \widetilde{R}^*_{\text{in}} \quad (7)$$

$$R^*_{in} + M \xrightarrow{k_1} R^*_1 \quad (8)$$

$$\widetilde{R}^*_{\text{in}} + M \xrightarrow{k_2} \widetilde{R}^*_1 \quad (9)$$

$$\widetilde{P}_r \xrightarrow{k_{d2}} R^*_{\text{in}} + R^*_r \quad (10)$$

$$\widetilde{\widetilde{P}}_r \xrightarrow{2k_{d2}} R^*_{\text{in}} + \widetilde{R}^*_r \quad (11)$$

$$3M \xrightarrow{k_{\text{ia}}} 2R^*_1 \quad (12)$$

Propagation

$$R^*_r + M \xrightarrow{k_p} R^*_{r+1} \quad (13)$$

$$\widetilde{R}^*_r + M \xrightarrow{k_p} \widetilde{R}^*_{r+1} \quad (14)$$

Termination
Combination

$$R^*_r + R^*_s \xrightarrow{k_{\text{tc}}} P_{r+s} \quad (15)$$

$$R^*_r + \widetilde{R}^*_s \xrightarrow{k_{\text{tc}}} \widetilde{P}_{r+s} \quad (16)$$

$$\widetilde{R}^*_r + \widetilde{R}^*_s \xrightarrow{k_{\text{tc}}} \widetilde{\widetilde{P}}_{r+s} \quad (17)$$

Chain Transfer to Small Molecules

$$R^*_n + T \xrightarrow{k_{fT}} P_r + T^* \quad (18)$$

$$\widetilde{R}^*_n + T \xrightarrow{k_{fT}} \widetilde{P}_r + T^* \quad (19)$$

T = initiator, solvent, CTA, inhibitor or impurity.

The model wass built using the mass balance for each species and the method of moments to predict averages molecular weight.[5,9,12,14] Table II presents the model equations for polymerization reactions using mono- and bi-functional initiators.

RESULTS

Model validation

The results presented in this section show the simulation of styrene polymerization using BPO as monofunctional initiator and D162 and L256 as bifunc-tional initiators. Two different bifunctional initiators were used to better compare the behavior between mono- and bi-functional peroxides. D162 was chosen because it is the most suitable as a substitute for BPO and it is quite effective over a temperature range wider than that suitable for the L256 initiator, according to a previous study by Villalobos et al.[5] L256 was picked because it is one of the most studied bifunctional initiator for the styrene polymerization and its reactivity characteristics are known.[5] It has similar half life when compared to BPO, yet its advantage resides in producing polystyrene of higher molecular weight and speeding up the reaction.[9]

Figures 1 to 6 show some validation plots of the model using experimental data available in literature[9] for the polymerization with BPO, D162, and L256. More operating conditions were tested; however, just a few is shown in this article, for sake of space.

These results show that the model prediction presents good agreement with experimental data from literature. This will assure confidence in the results obtained from parametric studies that will be presented later. Dhib et al.[9] used different operating conditions for the three initiators; however, as their focus was the development of mathematical models, the results were shown in different graphs, not being clear the difference in performance of the three initiators.

The focus of our work is to compare the performances of the three initiators under various operating conditions; therefore, the first six graphs are just to show that the developed model is reliable.

Figures 7 and 8 present the dissociation rate constant of the three initiators to the break of the first O—O bond (k_d) and to the break of the second O—O bond (k_{d2}) versus temperature. L256 dissociates faster than BPO and D162 in the first bond and L256 dissociates faster than D162 in the second bond (only bifunctional initiators have the second group O—O).

To investigate the behavior of bifunctional initiators, simulations were performed to analyze the effects of the initiator concentration and temperature on the conversion and molecular weight profiles.

The effect of initial initiator concentration

Figures 9, 10, and 11 show simulation results of monomer conversions profiles using three different concentrations of initiators (0.01 mol/L, 0.005 mol/L, and 0.00125 mol/L).

Comparing BPO and L256 profiles, it can be observed that the reaction rate is faster when L256 is used. This can be explained by the fact that L256 generates more free radicals compared to BPO (see Fig. 7), as it has a faster dissociation rate constant. Besides, the L256 generates two types of free radicals (monoradicals and diradical).

Comparing conversion profiles when using D162 and BPO, it can be observed that they are very similar. Despite D162 generates four primary radicals (one diradical and two monoradicals) and BPO

TABLE II
Model Equations: Monofunctional Initiator

Mass balance for all species	
Monomer	$\frac{d(V[M])}{dt} = F_M^e - k_p[M][R^*]V - F_M^s - 2k_{ia}[M]^3V - k_{fM}[M][R^*]V$
Initiator	$\frac{d(V[I])}{dt} = F_I^e - fk_d[I]V - F_M^s$
Polymer	$\frac{d(V[P])}{dt} = F_P^e + k_p[M][R^*]V - F_P^s$
Solvent	$\frac{d(V[S])}{dt} = F_S^e - k_{fS}[S][R^*]V - F_S^s$
Inhibitor or impurity	$\frac{d(V[Z])}{dt} = F_Z^e - k_{fZ}[Z][R^*]V - F_Z^s$
CTA	$\frac{d(V[CTA])}{dt} = F_{CTA}^e - k_{fCTA}[CTA][R^*]V - F_{CTA}^s$
Free radical	$\frac{d(V[R^*])}{dt} = 2fk_d[I]V + 2k_{ia}[M]^3V - k_{tc}[R^*]^2V - k_{fZ}[Z][R^*]V$
Total radical concentration	$\lambda_{to} = \lambda_0$ (radical type R^*)
Method of moments	
Zeroth moment of live radical distribution (λ_0)	$\frac{1}{V}\frac{d(V\lambda_0)}{dt} = 2fk_d[I] - k_{tc}\lambda_0\lambda_{to} - k_{fZ}\lambda_0[Z] + 2k_{ia}[M]^3 - \frac{q\lambda_0}{V}$
First moment of live radical distribution (λ_1)	$\frac{1}{V}\frac{d(V\lambda_1)}{dt} = 2fk_d[I] - k_{fZ}\lambda_1[Z] + 2k_{ia}[M]^3 + k_p[M]\lambda_0 - k_{tc}\lambda_0\lambda_1 + k_{fM}[M](\lambda_0 - \lambda_1) + k_{fS}[S](\lambda_0 - \lambda_1) + k_{fCTA}[CTA](\lambda_0 - \lambda_1) - \frac{q\lambda_1}{V}$
Second moment of live radical distribution (λ_2)	$\frac{1}{V}\frac{d(V\lambda_2)}{dt} = 2fk_d[I] - k_{fZ}\lambda_2[Z] + 2k_{ia}[M]^3 + k_p[M](2\lambda_1 + \lambda_0) - k_{tc}\lambda_0\lambda_2 + k_{fM}[M](\lambda_0 - \lambda_2) + k_{fS}[S](\lambda_0 - \lambda_2) + k_{fCTA}[CTA](\lambda_0 - \lambda_2) - \frac{q\lambda_2}{V}$
Zeroth moment of dead polymer distribution (μ_0)	$\frac{1}{V}\frac{d(V\mu_0)}{dt} = \frac{1}{2}k_{tc}\lambda_0^2 + k_{fM}\lambda_0[M] + k_{fS}\lambda_0[S] + k_{fCTA}\lambda_0[CTA] + k_{fZ}\lambda_0[Z] - \frac{q\mu_0}{V}$
First moment of dead polymer distribution (μ_1)	$\frac{1}{V}\frac{d(V\mu_1)}{dt} = k_{tc}\lambda_0\lambda_1 + k_{fM}\lambda_1[M] + k_{fS}\lambda_1[S] + k_{fCTA}\lambda_1[CTA] + k_{fZ}\lambda_1[Z] - \frac{q\mu_1}{V}$
Second moment of dead polymer distribution (μ_2)	$\frac{1}{V}\frac{d(V\mu_2)}{dt} = k_{tc}(\lambda_0\lambda_2 + \lambda_1^2) + k_{fM}\lambda_2[M] + k_{fS}\lambda_2[S] + k_{fCTA}\lambda_2[CTA] + k_{fZ}\lambda_2[Z] - \frac{q\mu_2}{V}$

Number average molecular weight	$\overline{M}_N = MW\frac{\mu_1}{\mu_0}$
Weight average molecular weight	$\overline{M}_W = MW\frac{\mu_2}{\mu_1}$

Model Equations: Bifunctional Initiator

Mass balance for all species	
Monomer	$\frac{d(V[M])}{dt} = F_M^e - k_p[M]\lambda_{to}V - F_M^s - 2k_{ia}[M]^3V - k_{fM}[M]\lambda_{to}V$
Initiator	$\frac{d(V[I])}{dt} = F_I^e - 2fk_{d1}[I]V - F_M^s$
Solvent	$\frac{d(V[S])}{dt} = F_S^e - k_{fS}[S]\lambda_{to}V - F_S^s$
Inhibitor or impurity	$\frac{d(V[Z])}{dt} = F_Z^e - k_{fZ}[Z]\lambda_{to}V - F_Z^s$
CTA	$\frac{d(V[CTA])}{dt} = F_{CTA}^e - k_{fCTA}[CTA]\lambda_{to}V - F_{CTA}^s$
Total radical concentration	$\lambda_{to} = \lambda_o + \widetilde{\lambda}_o$ (radicals types R^* and $\widetilde{R}*$)
Method of moments	
Zeroth moment of live radical distribution (λ_0)	$\frac{1}{V}\frac{d(V\lambda_0)}{dt} = 2f_1k_{d1}[I] + f_2k_{d2}\left(2\widetilde{\mu}_0 + 2\widetilde{\widetilde{\mu}}_0\right) + 2k_{ia}M^3 + k_{fM}[M]\widetilde{\lambda}_0 + k_{fS}[S]\widetilde{\lambda}_0 + k_{fCTA}[CTA]\widetilde{\lambda}_0 - k_{tc}\lambda_0\lambda_{to} - k_{fZ}[Z]\lambda_0 - \frac{q\lambda_0}{V}$
Zeroth moment of live radical distribution ($\widetilde{\lambda}_0$)	$\frac{1}{V}\frac{d(V\widetilde{\lambda}_0)}{dt} = 2f_1k_{d1}[I] + 2f_2k_{d2}\widetilde{\widetilde{\mu}}_0 - k_{fM}[M]\widetilde{\lambda}_0 - k_{fS}[S]\widetilde{\lambda}_0 - k_{fCTA}[CTA]\widetilde{\lambda}_0 - k_{tc}\lambda_{to}\widetilde{\lambda}_0 - k_{fZ}[Z]\widetilde{\lambda}_0 - \frac{q\widetilde{\lambda}_0}{V}$
First moment of live radical distribution (λ_1)	$\frac{1}{V}\frac{d(V\lambda_1)}{dt} = 2f_1k_{d1}[I] + f_2k_{d2}(\widetilde{\mu}_0 + 2\widetilde{\widetilde{\mu}}_0 + \widetilde{\mu}_1) + 2k_{ia}M^3 - k_{fZ}[Z]\lambda_1 - k_{tc}\lambda_{to}\lambda_1 + k_{fM}[M](\lambda_{to} - \lambda_1) + k_{fS}(\lambda_{to} - \lambda_1) + k_{fCTA}[CTA](\lambda_{to} - \lambda_1) + k_P[M]\lambda_0 - \frac{q\lambda_1}{V}$
First moment of live radical distribution ($\widetilde{\lambda}_1$)	$\frac{1}{V}\frac{d(V\widetilde{\lambda}_1)}{dt} = 2f_1k_{d1}[I] + 2f_2k_{d2}\widetilde{\widetilde{\mu}}_1 - k_Z\widetilde{\lambda}_1[Z] + k_p[M]\widetilde{\lambda}_0 - k_{tc}\lambda_{to}\widetilde{\lambda}_1 - k_{fM}[M]\widetilde{\lambda}_1 - k_{fS}[S]\widetilde{\lambda}_1 - k_{fCTA}[CTA]\widetilde{\lambda}_1 - \frac{q\widetilde{\lambda}_1}{V}$
Second moment of live radical distribution (λ_2)	$\frac{1}{V}\frac{d(V\lambda_2)}{dt} = 2f_1k_{d1}[I] + f_2k_{d2}(\widetilde{\mu}_0 + 2\widetilde{\widetilde{\mu}}_0 + \widetilde{\mu}_2) + 2k_{ia}M^3 - k_Z\lambda_2[Z] + k_p[M] \times (2\lambda_1 + \lambda_0) - k_{tc}\lambda_{to}\lambda_2 + -k_{fM}[M]\lambda_2 - k_{fS}[S]\lambda_2 - k_{fCTA}[CTA]\lambda_2 - \frac{q\lambda_2}{V}$

Second moment of live radical distribution ($\widetilde{\lambda}_2$)

$$\frac{1}{V}\frac{d(V\widetilde{\lambda}_2)}{dt} = 2f_1k_{d1}[I] + 2f_2k_{d2}\widetilde{\widetilde{\mu}}_2 - k_Z\widetilde{\lambda}_2[Z] + k_p[M]\left(2\widetilde{\lambda}_1 + \widetilde{\lambda}_0\right) - k_{tc}\lambda_{to}\widetilde{\lambda}_2 - k_{fM}[M]\widetilde{\lambda}_2 - k_{fS}[S]\widetilde{\lambda}_2 - k_{fCTA}[CTA]\widetilde{\lambda}_2 - \frac{q\widetilde{\lambda}_2}{V}$$

Zeroth moment of dead polymer distribution (μ_0)

$$\frac{1}{V}\frac{d(V\mu_0)}{dt} = \frac{1}{2}k_{tc}\lambda_0^2 + k_{fM}\lambda_0[M] + k_{fS}\lambda_0[S] + k_{fCTA}\lambda_0[CTA] + k_{fZ}\lambda_0[Z] - \frac{q\mu_0}{V}$$

First moment of dead polymer distribution (μ_1)

$$\frac{1}{V}\frac{d(V\mu_1)}{dt} = k_{tc}\lambda_0\lambda_1 + k_{fM}\lambda_1[M] + k_{fS}\lambda_1[S] + k_{fCTA}\lambda_1[CTA] + k_{fZ}\lambda_1[Z] - \frac{q\mu_1}{V}$$

Second moment of dead polymer distribution (μ_2)

$$\frac{1}{V}\frac{d(V\mu_2)}{dt} = k_{tc}(\lambda_0\lambda_2 + \lambda_1^2) + k_{fM}\lambda_2[M] + k_{fS}\lambda_2[S] + k_{fCTA}\lambda_2[CTA] + k_{fZ}\lambda_2[Z] - \frac{q\mu_2}{V}$$

Zeroth moment of temporary polymer distribution ($\widetilde{\mu}_0$)

$$\frac{1}{V}\frac{d(V\widetilde{\mu}_0)}{dt} = -k_{d2}\widetilde{\mu}_0 + k_{tc}\lambda_0\widetilde{\lambda}_0 + k_{fM}\widetilde{\lambda}_0[M] + k_{fS}\widetilde{\lambda}_0[S] + k_{fCTA}\widetilde{\lambda}_0[CTA] + k_{fZ}\widetilde{\lambda}_0[Z] - \frac{q\widetilde{\mu}_0}{V}$$

First moment of temporary polymer distribution ($\widetilde{\mu}_1$)

$$\frac{1}{V}\frac{d(V\widetilde{\mu}_1)}{dt} = -k_{d2}\widetilde{\mu}_1 + k_{tc}(\lambda_0\widetilde{\lambda}_1 + \lambda_1\widetilde{\lambda}_0) + k_{fM}\widetilde{\lambda}_1[M] + k_{fS}\widetilde{\lambda}_1[S] + k_{fCTA}\widetilde{\lambda}_1[CTA] + k_{fZ}\widetilde{\lambda}_1[Z] - \frac{q\widetilde{\mu}_1}{V}$$

Second moment of temporary polymer distribution ($\widetilde{\mu}_2$)

$$\frac{1}{V}\frac{d(V\widetilde{\mu}_2)}{dt} = -k_{d2}\widetilde{\mu}_2 + k_{tc}(\lambda_0\widetilde{\lambda}_2 + 2\lambda_1\widetilde{\lambda}_1 + \lambda_0\widetilde{\lambda}_2) + k_{fM}\widetilde{\lambda}_2[M] + k_{fS}\widetilde{\lambda}_2[S] + k_{fCTA}\widetilde{\lambda}_2[CTA] + k_{fZ}\widetilde{\lambda}_2[Z] - \frac{q\widetilde{\mu}_2}{V}$$

Zeroth moment of temporary polymer distribution ($\widetilde{\widetilde{\mu}}_0$)

$$\frac{1}{V}\frac{d(V\widetilde{\widetilde{\mu}}_0)}{dt} = -2k_{d2}\widetilde{\widetilde{\mu}}_0 + k_{tc}\widetilde{\lambda}_0^2 - \frac{q\widetilde{\widetilde{\mu}}_0}{V}$$

First moment of temporary polymer distribution ($\widetilde{\widetilde{\mu}}_1$)

$$\frac{1}{V}\frac{d(V\widetilde{\widetilde{\mu}}_1)}{dt} = -2k_{d2}\widetilde{\widetilde{\mu}}_1 + k_{tc}\widetilde{\lambda}_0\widetilde{\lambda}_1 - \frac{q\widetilde{\widetilde{\mu}}_1}{V}$$

Second moment of temporary polymer distribution ($\widetilde{\widetilde{\mu}}_2$)

$$\frac{1}{V}\frac{d(V\widetilde{\widetilde{\mu}}_2)}{dt} = -2k_{d2}\widetilde{\mu}_2 + k_{tc}\widetilde{\lambda}_0\widetilde{\lambda}_2 + k_{tc}\widetilde{\lambda}_1^2 - \frac{q\widetilde{\widetilde{\mu}}_2}{V}$$

Number average molecular weight

$$\overline{M}_N = \frac{MW\{\mu_1 + \widetilde{\mu}_1 + \widetilde{\widetilde{\mu}}_1 + \lambda_1 + \widetilde{\lambda}_1\}}{\mu_0 + \widetilde{\mu}_0 + \widetilde{\widetilde{\mu}}_0 + \lambda_0 + \widetilde{\lambda}_0}$$

Weight average molecular weight

$$\overline{M}_W = \frac{MW\{\mu_2 + \widetilde{\mu}_2 + \widetilde{\widetilde{\mu}}_2 + \lambda_2 + \widetilde{\lambda}_2\}}{\mu_1 + \widetilde{\mu}_1 + \widetilde{\widetilde{\mu}}_1 + \lambda_1 + \widetilde{\lambda}_1}$$

generates only two primary radicals (two monoradicals), BPO has a higher dissociation rate constant (see Fig. 7), generating more monoradicals when compared to the D162. As the rate of the break of the second O—O bond (k_{d2}) for the D162 initiator is also low (see the low value of kd2 for the D162 in Fig. 8), the total amount of radicals (mono- and diradicals) generated when using D162 is similar to the amount of monoradicals generated when using BPO, resulting in similar profiles of conversion.

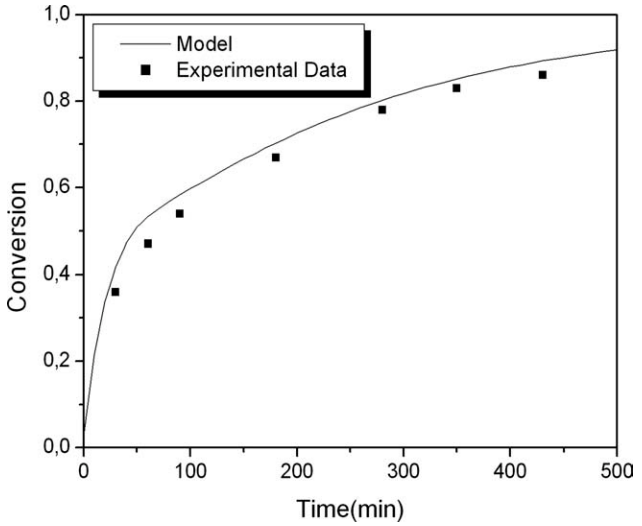

Figure 1 Polystyrene-conversion versus time (120°C, [BPO] = 0.01 mol/L).

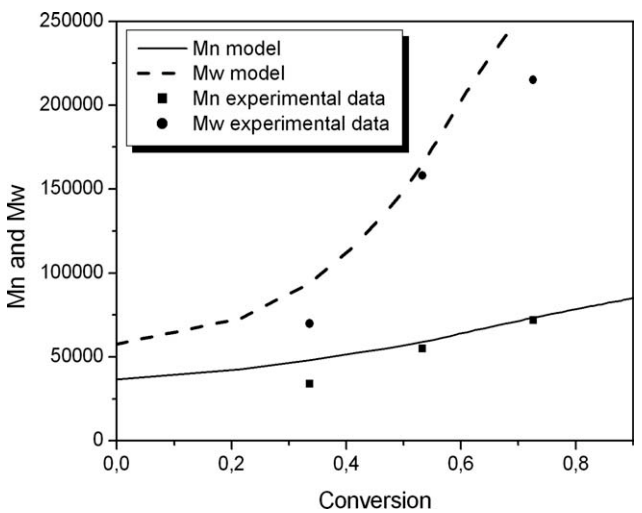

Figure 2 Polystyrene-Mn and Mw verses conversion (120°C, [BPO] = 0.01 mol/L).

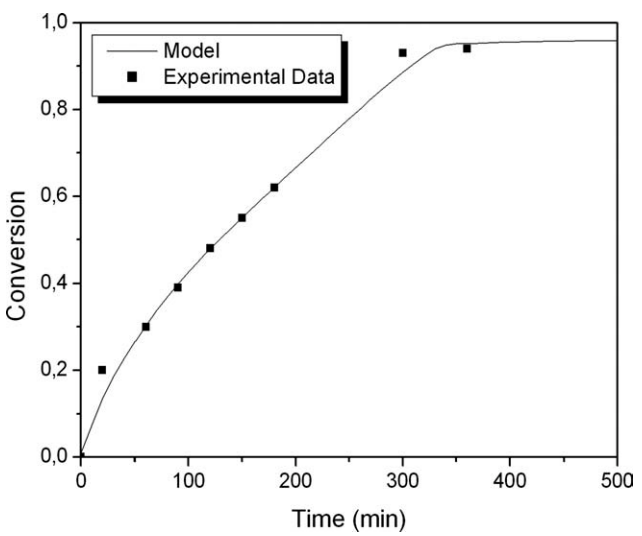

Figure 3 Polystyrene-conversion versus time (90°C, [L256] = 0.01 mol/L).

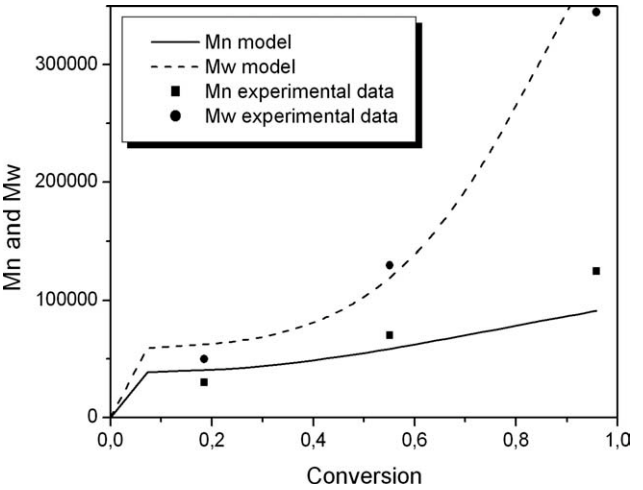

Figure 4 Polystyrene-Mn and Mw verses conversion (90°C, [L256] = 0.01 mol/L).

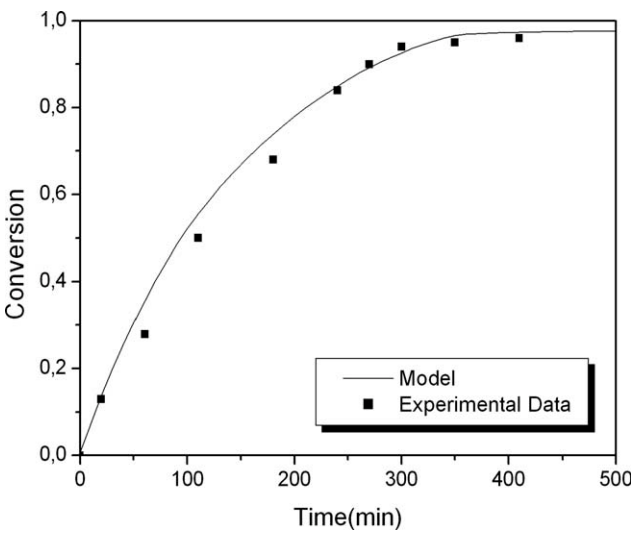

Figure 5 Polystyrene-conversion versus time (105°C, [L256] = 0.005 mol/L).

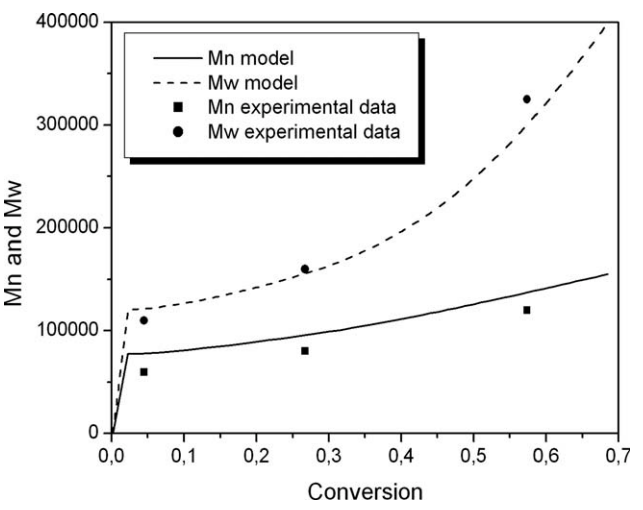

Figure 6 Polystyrene-Mn and Mw verses conversion (105°C, (L256) = 0.005 mol/L).

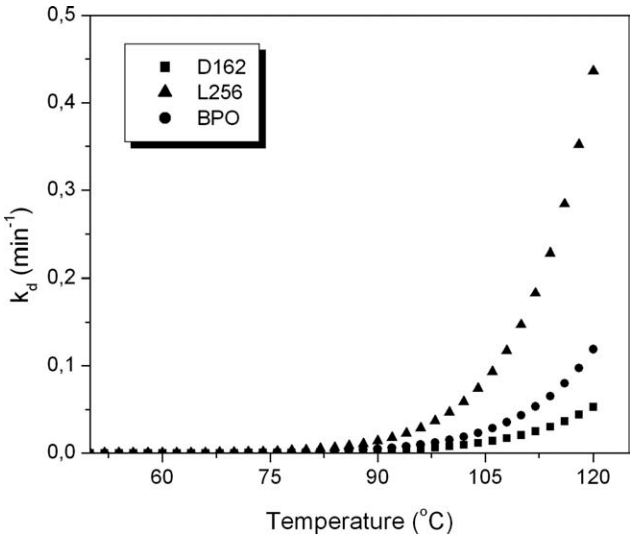

Figure 7 k_d versus Temperature.

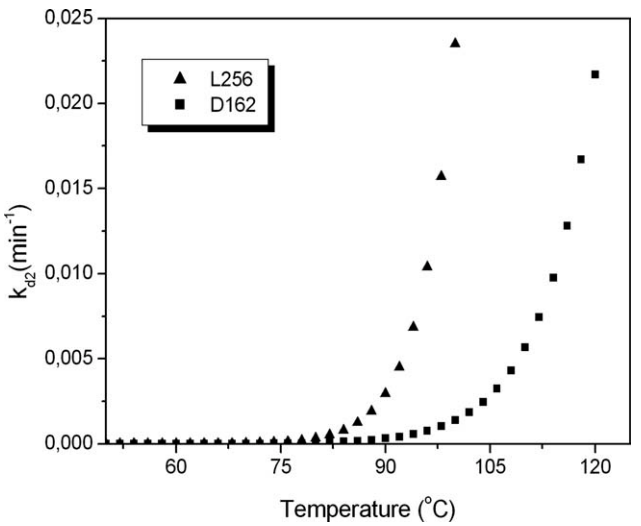

Figure 8 k_{d2} versus Temperature.

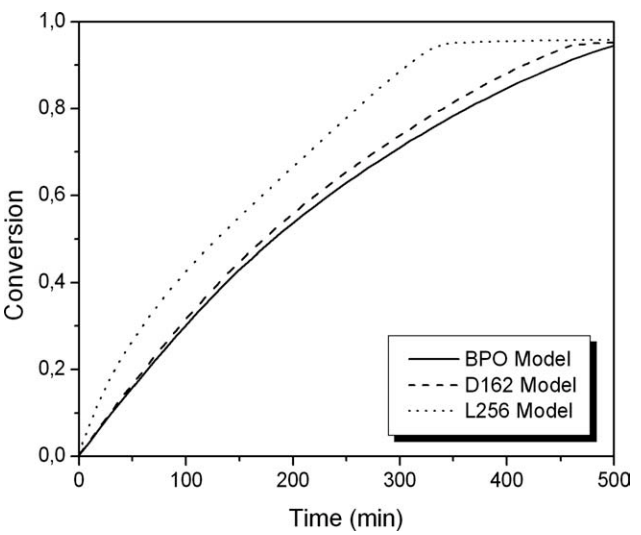

Figure 9 Polystyrene-conversion versus time (90°C, [*I*] = 0.01 mol/L).

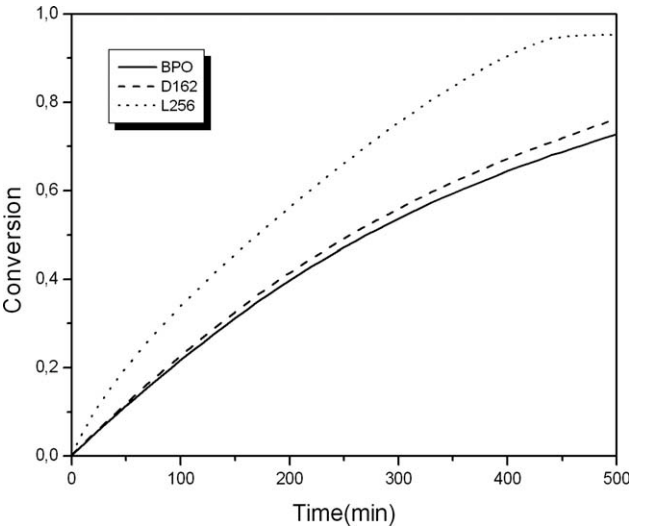

Figure 10 Polystyrene-conversion versus time (90°C, [*I*] = 0.005 mol/L).

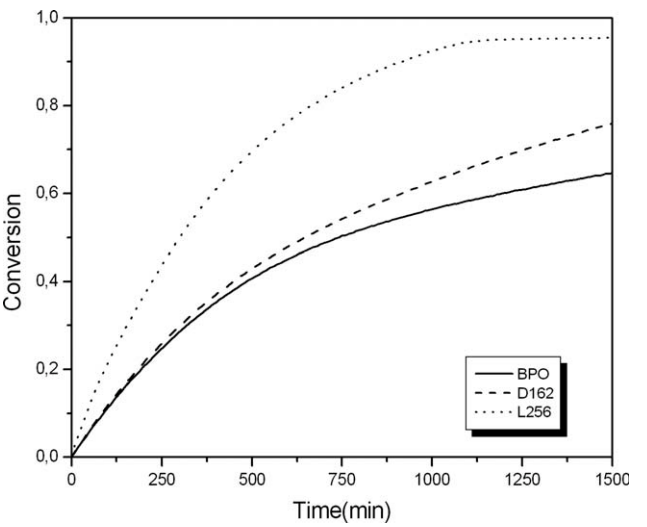

Figure 11 Polystyrene-conversion versus time (90°C, [*I*] = 0.00125 mol/L).

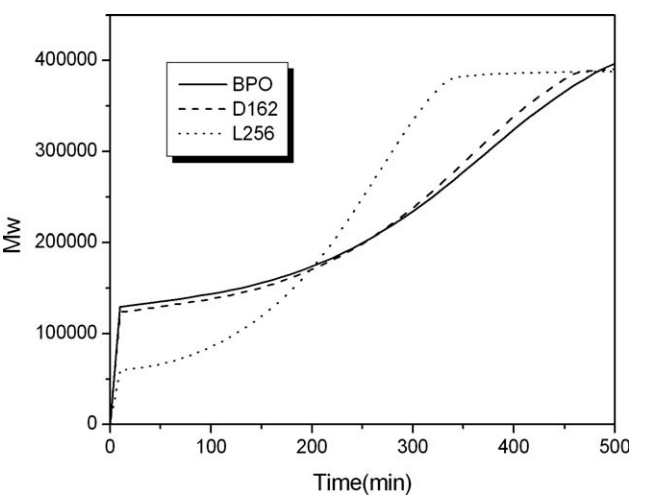

Figure 12 Polystyrene-M_w versus time (90°C, [*I*] = 0.01 mol/L).

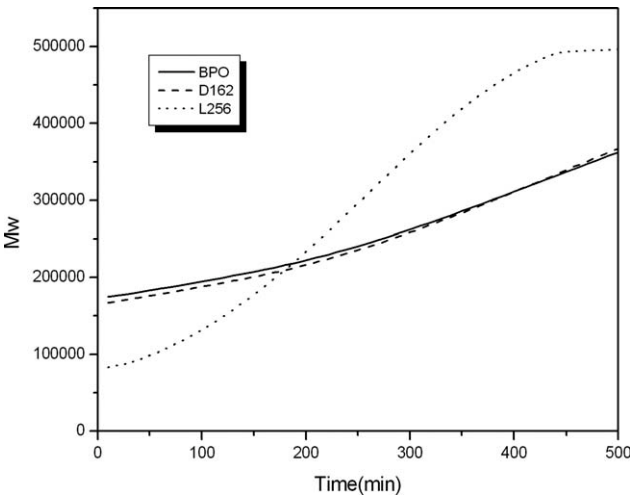

Figure 13 Polystyrene-M_w versus time (90°C, [I] = 0.005 mol/L).

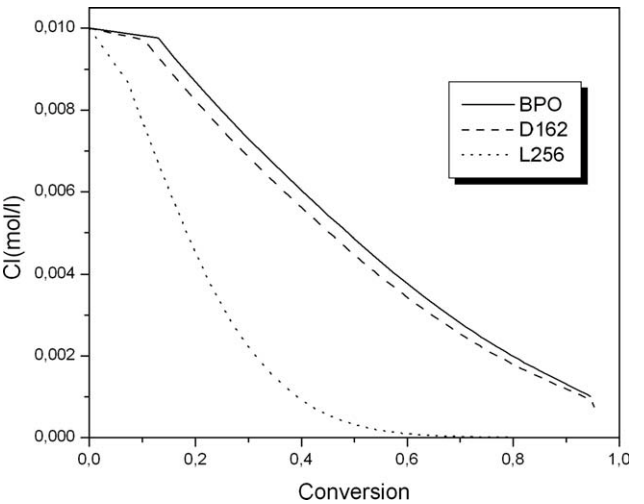

Figure 15 Initiator concentration versus conversion (90°C, [I] = 0.01 mol/L).

Figures 10, 12, and 14 show simulation results of weight average molecular weight obtained using the three initiators. BPO and D162 profiles are very close, due to the values of dissociation rate constant, as explained before. Comparing M_w profiles obtained from BPO and L256 initiators, it can be observed that L256 presents higher molecular weight at the end of the polymerization, despite the fact of presenting higher conversions (see Figs. 9, 10, and 11). The effect of the two radicals in the same initiator fragment (chain growth on both sides of the fragment, increasing the molecular weight and the reaction rate simultaneously) can be clearly observed here.

Figures 15, 16, and 17 show simulation results of initiator concentration for the three initiators. It can be noticed that only for the smallest initiator concentration (0.00125 mol/L), the three initiators are totally consumed. In this case, a more efficient break of the second O—O bond of bifunctional initiators occurs, and as a result, the conversion profiles using BPO and D162 start being more different (Fig. 11) and the M_w obtained from L256 becomes higher as the beginning of the reaction (Fig. 14).

It can be clearly observed that the difference between mono- and bi-functional initiators becomes more evident as the initial initiator concentration becomes smaller, due to the second O—O bond being preferentially broken when the initiator concentration is small (the second O—O bond starts breaking more easily when the first O—O bond is already broken).

Besides conversion, molecular weight, and initiator concentration values, this model also predicts results such as radical concentration, polydispersity index (PDI), and moments of live and dead

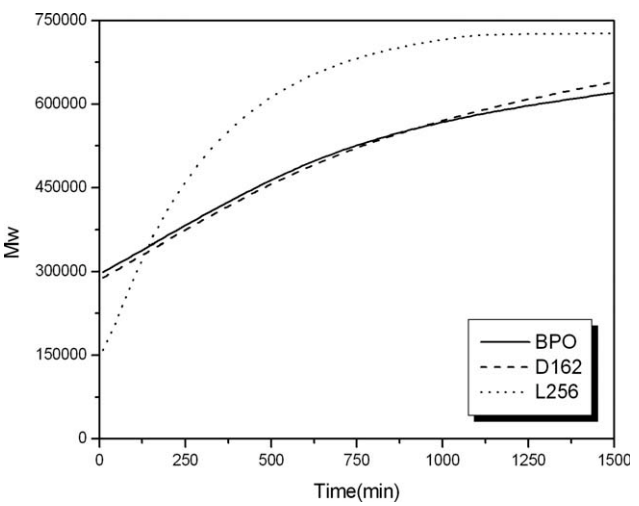

Figure 14 Polystyrene-M_w versus time (90°C, [I] = 0.00125 mol/L).

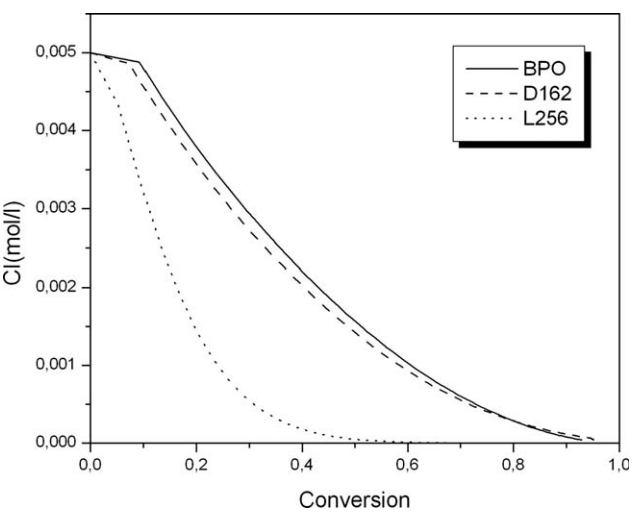

Figure 16 Initiator concentration versus conversion (90°C, [I] = 0.005 mol/L).

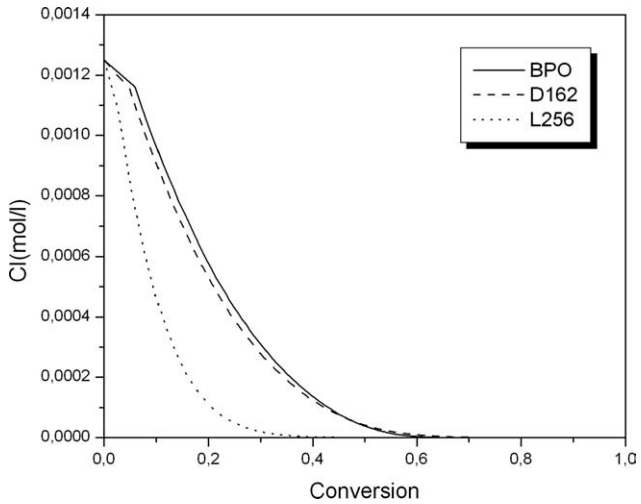

Figure 17 Initiator concentration versus conversion (90°C, $[I] = 0.00125$ mol/L).

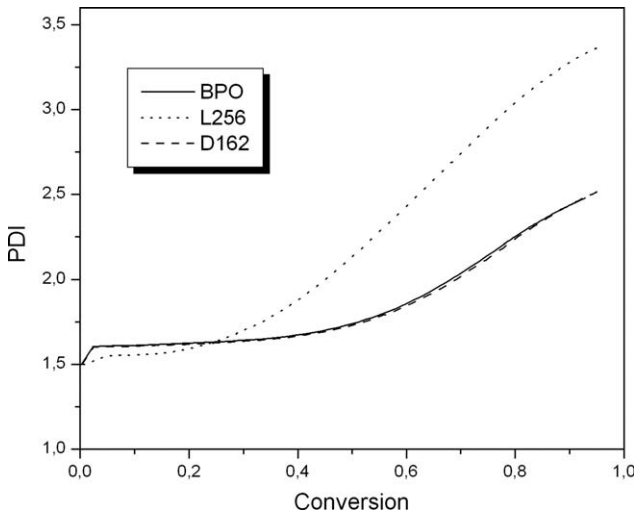

Figure 19 Polydispersity index versus conversion, (90°C, $[I] = 0.005$ mol/L).

polymers. Figures 18, 19, and 20 show simulation results of PDI versus conversion. It is possible to verify the difference between the monofunctional initiator and the two bifunctional initiators. This was expected as the molecular weight values from polymers generated by bifunctional initiators are greater than those from monofunctional initiators.

Figures 21 to 26 show simulation profiles of radical concentration and moments of live and dead polymers. For the monofunctional initiator BPO, the moment of live polymer λ_0 is the radical concentration ($\lambda_{total} = RC = \lambda_0$, see Figs. 21 and 22). However, the profiles are not the same for bifunctional initiators. This happens because the radical concentration is the summation of the moment of live polymer and the moment of live polymer with one undecomposed peroxide group ($\lambda_{total} = \lambda_0 + \widetilde{\lambda}_0$). It can be also verified in Figure 23 that at a very high initiator concentration ($[I] = 0.01$ mol/L), the presence of radicals with unbroken O—O bonds is very small, as the radical concentration and λ_0 profiles are very similar, see Figures 21 and 22 (radical concentration and λ_0 values are in the same order of magnitude, and their difference is $\widetilde{\lambda}_0$).

Figure 24 presents the moment of dead polymer profile. It can be noticed that the monofunctional initiator BPO produces a higher amount of polymer compared to the two bifunctional initiators, D162 and L256. This happens because BPO does not have radicals with undecomposed peroxides, so termination reactions only form dead polymers (μ_0) and there is no formation of any other type of polymer (intermediate polymers, $\widetilde{\mu}_0$ and $\widetilde{\widetilde{\mu}}_0$) as there is in the case of bifunctional initiators.

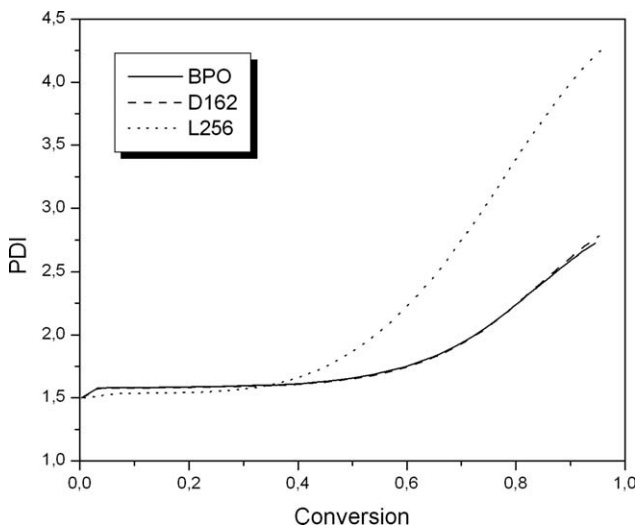

Figure 18 Polydispersity index versus conversion (90°C, $[I] = 0.01$ mol/L).

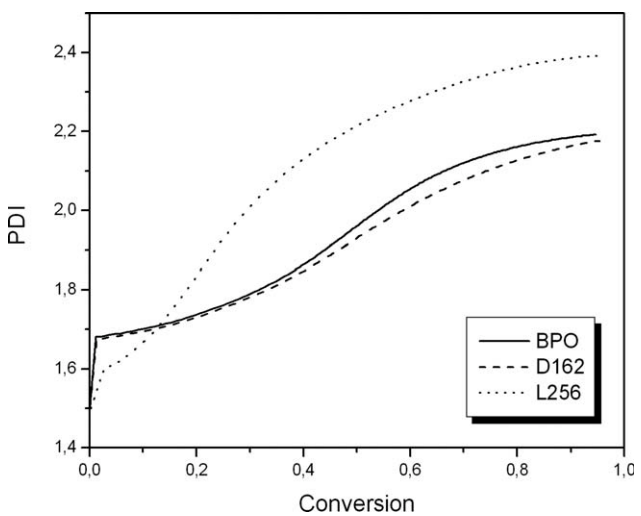

Figure 20 Polydispersity index versus conversion, (90°C, $[I] = 0.00125$ mol/L).

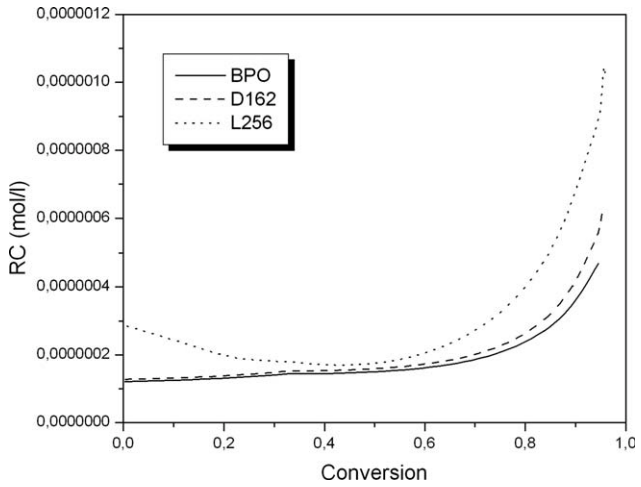

Figure 21 Radical concentration versus conversion (90°C, $[I] = 0.01$ mol/L).

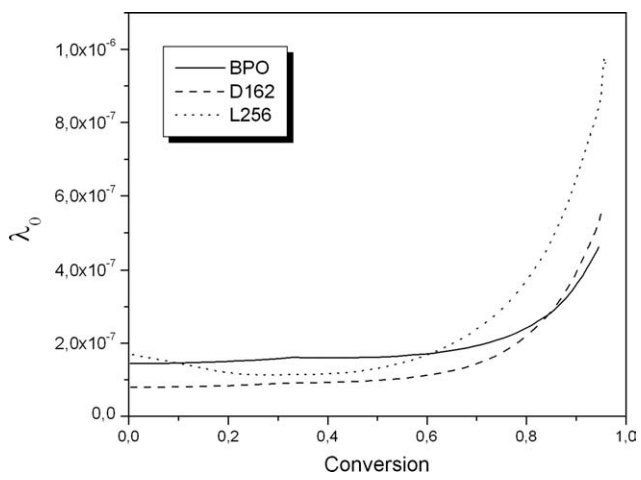

Figure 22 Moment of live polymer, λ_0, versus conversion (90°C, $[I] = 0.01$ mol/L).

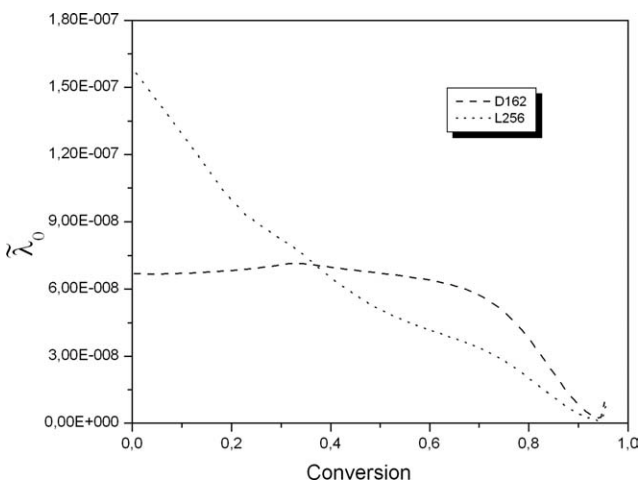

Figure 23 Moment of live polymer with one undecomposed peroxide, $\tilde{\lambda}_0$, versus conversion (90°C, $[I] = 0.01$ mol/L).

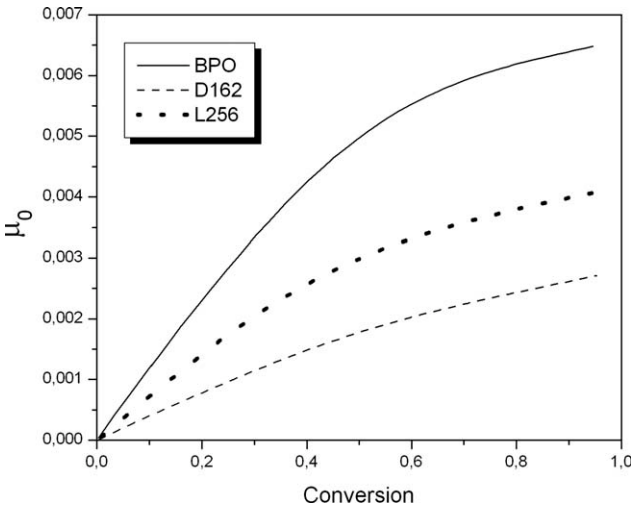

Figure 24 Moment of dead polymer, μ_0, versus conversion (90°C, $[I] = 0.01$ mol/L).

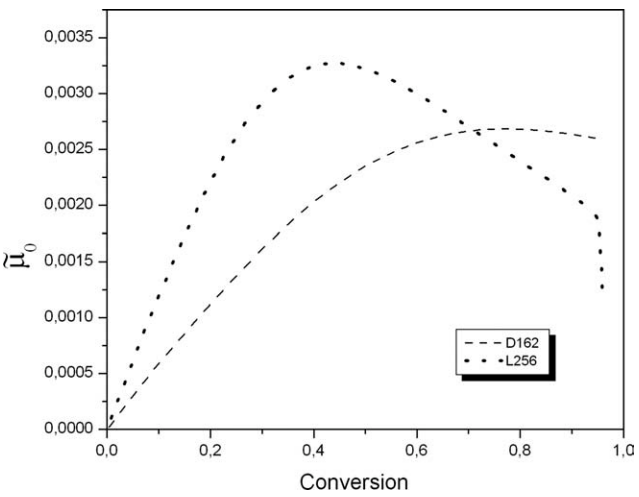

Figure 25 Moment of intermediate polymer with one undecomposed peroxide, $\tilde{\mu}_0$, versus conversion (90°C, $[I] = 0.01$ mol/L).

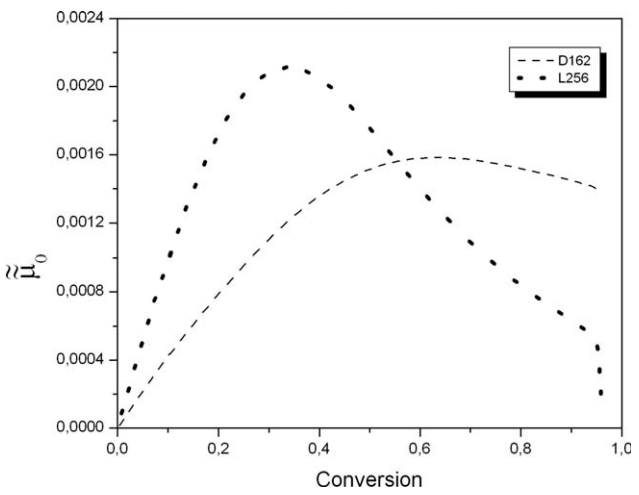

Figure 26 Moment of intermediate polymer with two undecomposed peroxides, $\tilde{\tilde{\mu}}_0$, versus conversion (90°C, $[I] = 0.01$ mol/L).

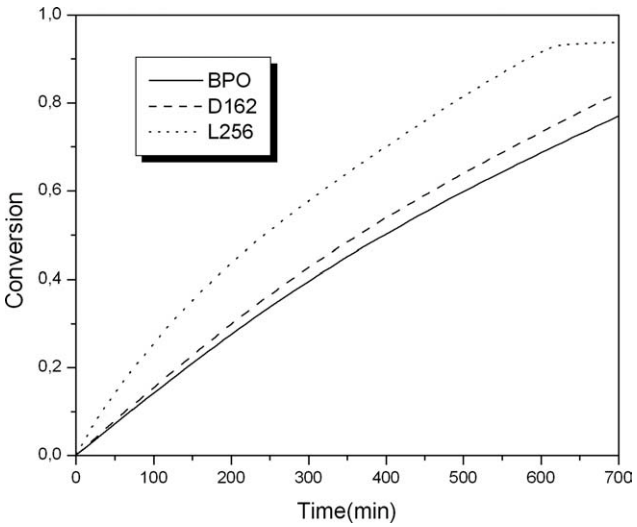

Figure 27 Polystyrene-conversion versus time (80°C, [*I*] = 0.01 mol/L).

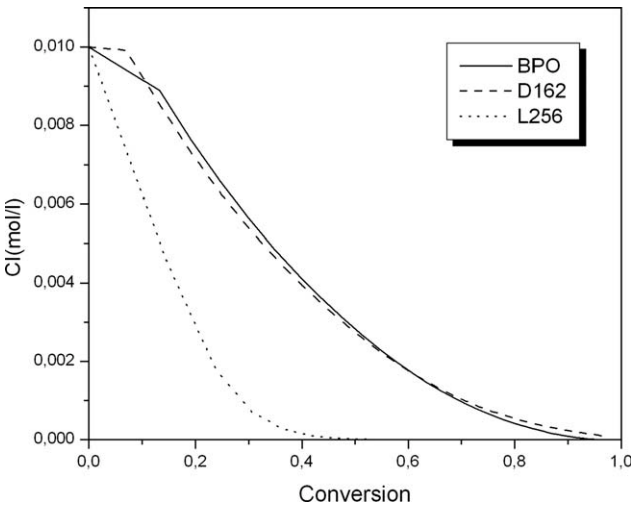

Figure 29 Initiator concentration versus conversion (100°C, [*I*] = 0.01 mol/L).

These intermediate polymers ($\widetilde{\mu}_0$ and $\widetilde{\widetilde{\mu}}_0$) are macromolecules with still not broken O—O bonds. As the initiator is consumed, these peroxides groups start breaking, providing a new growth of the chain that generates dead polymers with very high molecular weight. Because of this, it is possible to verify in Figures 25 and 26 that $\widetilde{\mu}_0$ and $\widetilde{\widetilde{\mu}}_0$ values decrease as the conversion increases. A faster decrease in the profile can also be noticed when using the bifunctional initiator L256. That might occur due to the fact that the decomposition of L256 is faster.

Analyzing Figures 24, 25, and 26, it is possible to verify that the values of μ_0, $\widetilde{\mu}_0$, and $\widetilde{\widetilde{\mu}}_0$ profiles versus conversion are in the same order of magnitude, showing that for bifunctional initiators there is a significant quantity of polymers with undecomposed peroxide (O—O bonds). Apparently, the O—O bonds that are present in the intermediate polymers only start breaking when the initiator concentration is very low.

The effect of temperature

Figures 9, 12, and 27 to 30 show simulation results of the effect of the temperature on conversion and weight average molecular weight. The behavior of the three initiators was analyzed at 80°C, 90°C, and 100°C temperatures. As expected, it is possible to verify from Figures 9, 27, and 28 that the reaction rate increases with the temperature; however, at the highest temperature (T = 100°C, Fig. 28), the conversion profiles are similar for the three initiators used. This can be explained analyzing the initiator concentration profiles for the three initiators at the 100°C

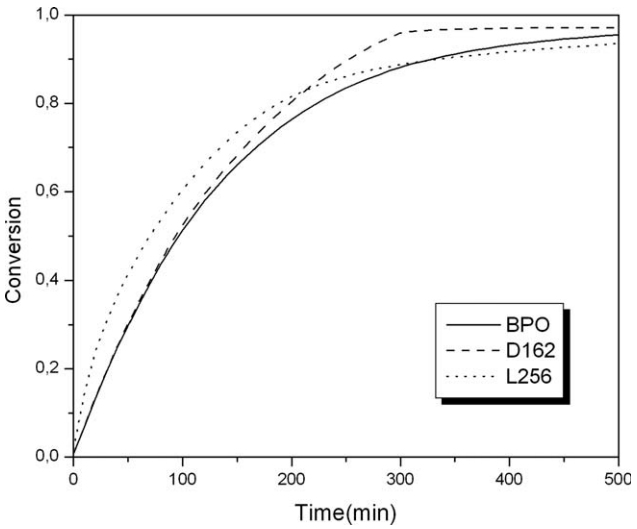

Figure 28 Polystyrene-conversion versus time (100°C, [*I*] = 0.01 mol/L).

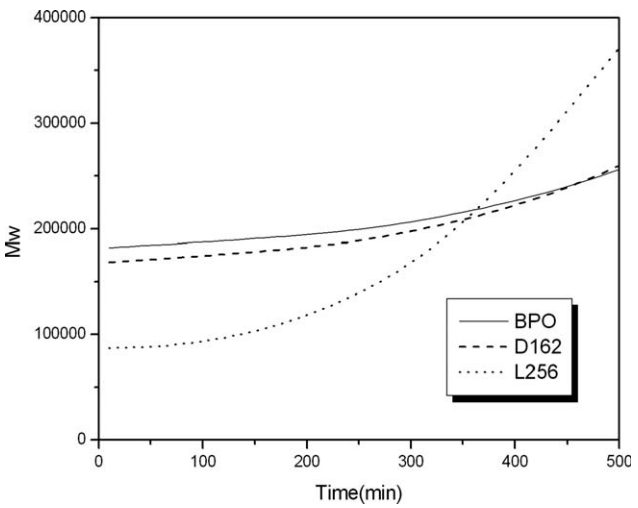

Figure 30 Polystyrene-M_w versus time (80°C, [*I*] = 0.01 mol/L).

temperature (Fig. 29). At 100°C, it can be noticed that the L256 initiator is completed consumed earlier, at monomer conversion around 60%, and its conversion profile is faster than the conversion profiles of D162 and BPO until 60%, but from this conversion, the three profiles become similar. So, maybe until 60% conversion, the first O—O bond of L256 is preferentially broken and after that, the second O—O bond is preferentially broken. In Figures 7 and 8, it is possible to verify that the L256 dissociation rate constant for the first O—O bond at 100°C is $k_d = 4.74 \times 10^{-2}$ min^{-1}, that is higher than the L256 dissociation rate constant for the second O—O bond, $k_{d2} = 2.26 \times 10^{-2}$ min^{-1}. This means that the production of new radicals, after 60% of conversion, is going to decrease in comparison with the production of radicals before 60%. Therefore, at 100°C, after a conversion of 60%, the consumption of monomer using L256 becomes slower making its conversion curve becomes closer to BPO and D162 curves.

Figures 12, 30, and 31 show simulation results of weight average molecular weight obtained using the three initiators. Profiles using the three initiators are very close at a high temperature. It has been observed that, in the beginning of the reaction, the weight average molecular weight obtained with L256 (higher k_d) is smaller than the weight average molecular weights obtained with D162 and BPO. The point where the three curves are close is characterized by the L256 total consumption that leads to the break of the second O—O bond (Figs. 15, 29, and 32).

CONCLUSION

Results from simulation of styrene polymerization using mono-functional (BPO), and bi-functional initiators (D162 and L256) showed good agreement with experimental data from literature, showing that the models are reliable and can be used to analyze and compare different types of initiators (mono- and bi-functional).

The conversion and molecular weight results show advantages in using L256 over BPO and D162, especially for the case when lower temperature and lower initial concentration of initiator were used (high molecular weight and high conversion were obtained, simultaneously).

The behavior obtained when using BPO and D162 was quite similar when an excess of initiator was used, due to the non-breakage of the second O—O bond (D162 was working as a monofunctional initiator) and due to the values of dissociation rates of the initiators.

It can be concluded that the advantages of using bifunctional initiators are directly related to the operating condition used during the polymerization.

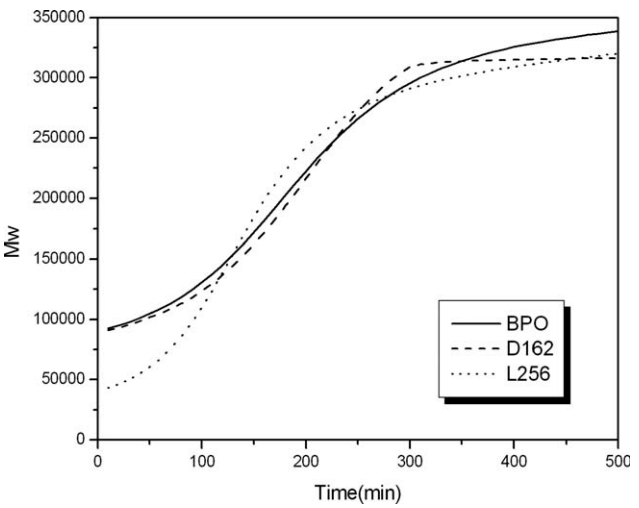

Figure 31 Polystyrene-M_w versus time (100°C, [I] = 0.01 mol/L).

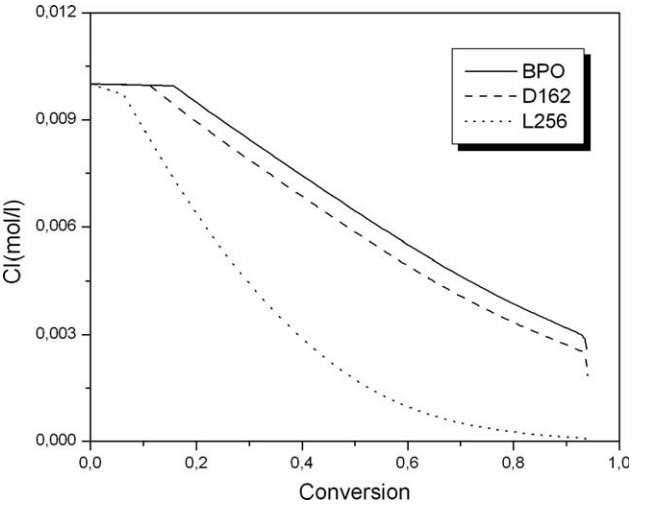

Figure 32 Initiator concentration versus conversion (80°C, [I] = 0.01 mol/L).

NOMENCLATURE

CTA	Chain transfer agent
I	Initiator
CI	Initiator concentration, mol/L
k_{ia}	Rate constant for thermal initiation, L^2/mol^2 min
k_d	Decomposition rate constant of monofunctional initiator
k_{d1}	Decomposition rate constant of bifunctional initiator, min^{-1}
k_{d2}	Decomposition rate constant of peroxide with undecomposed radical, min^{-1}
k_{fT}	Rate constant for transfer to "T" (T can be, solvent, monomer, CTA, inhibitor or impurity), L/mol s
k_p	Rate constant for propagation, L/mol s
k_t	Rate constant for termination, L/mol s

k_{tc} Rate constant for termination through combination, L/mol s
k_{td} Rate constant for termination through desproportion, L/mol s
M Monomer
M_w Molecular weight
$\overline{M}_w$ Weight average molecular weight
$\overline{M}_n$ Number average molecular weight
PDI Polidispersity index
P_r Dead polymer molecule
$\widetilde{P}_r$ Dead polymer molecule with one undecomposed peroxide
$\widetilde{\widetilde{P}}_r$ Dead polymer molecule with two undecomposed peroxide
RC Radical concentration
R^*_{in} Primary initiator radical fragment
$\widetilde{R}^*_{in}$ Initiator radical fragment with one undecomposed peroxide
$R^*_{r,s}$ Regular radical of chain length r and s, $r \geq 1$, $s \geq 1$
$\widetilde{R}^*_r$ Macroradical fragment of chain length r, with one undecomposed peroxide, $r \geq 1$
$\widetilde{R}^*_s$ Macroradical fragment of chain length s, with one undecomposed peroxide, $s \geq 1$
λ_i Moments of live polymer radical ($i = 0,1,2$)
$\widetilde{\lambda}_i$ Moments of live polymer radical with one undecomposed peroxide ($i = 0,1,2$)
λ_{to} Total radical concentration ($= \lambda_0 + \widetilde{\lambda}_0$)
μ_i Moments of dead polymer radical ($i = 0,1,2$)
$\widetilde{\mu}_i$ Moments of dead polymer radical with one undecomposed peroxide ($i = 0,1,2$)
$\widetilde{\widetilde{\mu}}_i$ Moments of dead polymer radical with two undecomposed peroxide ($i = 0,1,2$)

References

1. Gao, J.; Penlidis, A. J Macromol Sci Revs Macromol Chem Phys 1996, C36, 199.
2. Choi, K. Y.; Lei, G. D. AIChE J 1987, 33, 2067.
3. Choi, K. Y.; Liang, W. R.; Lei, G. D. J Appl Polym Sci 1988, 35, 1547.
4. Kim, K. J.; Liang, W.; Choi, K. Y. Ind Eng Chem Res 1989, 28, 131.
5. Villalobos, M. A.; Hamielec, A. E.; Wood, P. E. J Appl Polym Sci 1991, 42, 629.
6. Yoon, W. J.; Choi, K. Y. Polymer 1992, 33, 4582.
7. Yoon, W. J.; Choi, K. Y. J Appl Polym Sci 1992, 46, 1353.
8. González, I. M.; Meira, G. R.; Oliva, H. M. J Appl Polym Sci 1996, 59, 1015.
9. Dhib, R.; Gao, J.; Penlidis, A. Polym React Eng 2000, 8, 299.
10. Cavin, L.; Rouge, A.; Meyer, T.; Renken, A. Polymer 2000, 41, 3925.
11. Benbachir, M.; Benjelloun, D. Polymer 2001, 42, 7727.
12. Dhib, R.; Al-Nidaway, N. Chem Eng Sci 2002, 5, 2735.
13. Asteasuain, M.; Brandolin, A.; Sarmoria, C. Polymer 2004, 45, 321.
14. Machado, P. F. M. P. B., MSc Thesis, The State University of Campinas-Brazil, 2004.